# Optical Probe for the Real Time and Vectorial Analysis of the Electric Field Induced by Ionized Gazes

Farah Aljammal, G. Gaborit, Guillaume Revillod, Sylvain Iséni, Lionel Duvillaret

# Optical Probe for the Real Time and Vectorial Analysis of the Electric Field Induced by Ionized Gazes

F. Aljammal[1], G. Gaborit[1,2], Guillaume Revillod[2], Sylvain Iseni[3] and Lionel Duvillaret[2]

[1]*IMEP-LAHC, Université Savoie Mont-Blanc, France*
[2]*KAPTEOS, Alpespace, Sainte-Hélène du Lac, France*
[3]*GREMI, Université d'Orléans, France*

**Abstract:** We here present the potentialities of the electro-optic technique dedicated to the electric field characterization of plasmas. A fully dielectric and millimetre sized probe allows to measure each component of the electric field vector in real time from quasi DC up to several GHz.

**Keywords:** optical sensors, plasma diagnostic, intense field, electro-optics, electric field.

## 1. Introduction

Among all the relevant characteristics of a plasma, its associated electric (E) field behaviour is one of the critical parameter to be analysed. Current and voltage driven by the plasma source are usually measured [1], but are definitely not sufficient for an exhaustive analysis. Historically, charge density gives additional informations on the plasma and can be assessed thanks to Langmuir probe [2] or a plasma ion analyser. The non stationary magnetic field can be measured using a B-dot probe [3]. Concerning the E-field, numerical simulations [4,5] are mainly performed. Actually, there is a lack of available tool allowing the actual measurement in the vicinity or within the plasma.

We here demonstrate the ability of an electrooptic (EO) transducer to provide a complete analysis of the E-field vector induced by the voltage source initiating the ionization process as well as by the plasma itself. The performances of such a technique are in a complete agreement with the requirements for the plasma analysis. Indeed, the measurement bandwidth exceeds several GHz for real time measurement and can be extended up to the THz domain in equivalent time configuration [6-8]. The dynamic range is greater than 120 dB and ranges from less than 1 V/m to more than $10^6$ V/m [9,10]. The transverse spatial resolution is better than 1 mm$^2$. Finally, the probe includes no metal and is millimetre sized, thus leading to very weak perturbation on the field to be measured, so on the nominal behaviour of the plasma.

## 2. Electrooptic probe and setup

The optical probe is based on a non centrosymmetric crystal, acting as a linear transducer between the field vector components and its eigen refractive indices. A low noise laser beam (DFB, $\lambda$=1.5 $\mu$m) crosses the crystal forth and back and carries, via its polarization state, the information related to the E-field induced modification of the crystal indices. Polarization maintaining fibres allow the remote optical feeding of the EO probe which is connected to an optoelectronic unit. This latter one includes the laser source and also photodiodes ensuring the final conversion into a electrical signal, still proportional to the considered E-field vector component. The probe is packaged with a dielectric sheath to ensure the mechanical and optical integrity. Moreover, this sheath is multi-layered, to improve the adiabatic transition of the field between the outer media and the crystal transducer. The whole measurement scheme is transportable and the performances are not affected by the temperature variation. The probe can be mounted on translation stage to perform the E-field mapping. An example of probes implementation is illustrated in Fig.1.

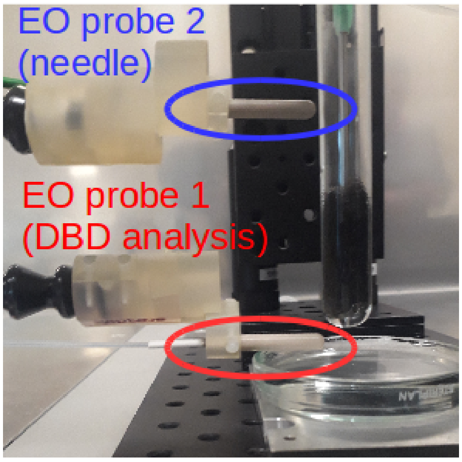


Fig. 1. Photography showing two EO probe located in the vicinity of dielectric barrier discharge reactor. Probe 1 analyses the discharges and probe 2 controls the radial field surrounding a high voltage fed needle. The grounded plane is at the bottom of the picture.

## 3. Experimental results

As an example, we here report some results concerning the analysis of dielectric barrier discharges (DBD). For that purpose, a needle is fed by a 50 Hz high voltage transformer (0.2-25 kVrms). The barriers consist in glass tube and glass plate for the anode and the cathode, respectively. Two probes are used to measure simultaneously the field in the vicinity of both needle and DBD. The obtained temporal waveforms of the radial (horizontal on Fig.1) field are shown in Fig.2. The behaviours of the field is analysed for two different feeding voltage. Fig.2a and Fig.2b corresponds to an applied voltage of 10 kVrms and 20 kVrms, respectively. The threshold of DBD appearance is here 16.5 kVrms, in agreement with the previously performed numerical expectations. The temporal evolution of all presented signals exhibits obviously the 50 Hz voltage signal.

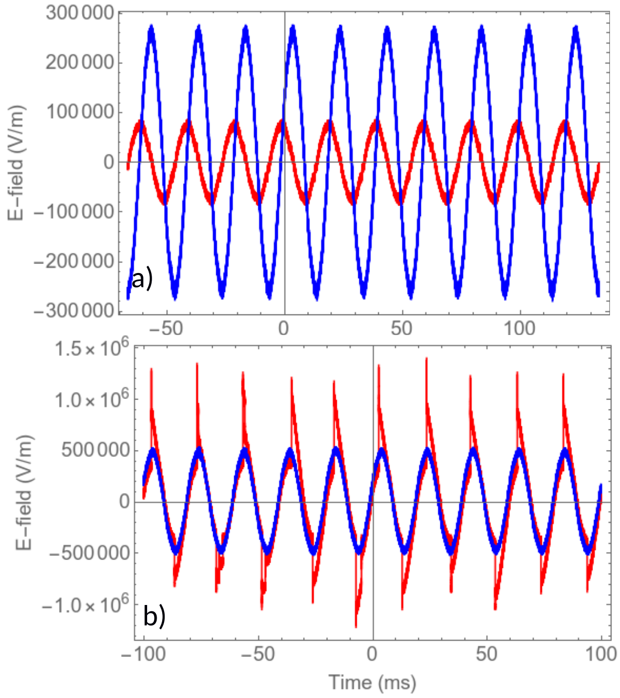


Fig. 2. a) Temporal evolution of the radial E-field in the vicinity of the needle (blue curve) and in between the needle and the ground plane (red curve). The feeding voltage is 10 kV, below the threshold voltage.
b) Temporal evolution of the radial E-field in the vicinity of the needle (blue curve) and very close to the DBD. the needle and the ground plane (red curve). The feeding voltage is 20 kV, above the threshold voltage. The inset is a picture of the DBD.

All the measured radial field values are in the 100 kV/m-1.5 MV/m range. When the applied voltage does not induce DBD (Fig.1a), the measurement in location of probe 1 shows a weaker signal than the probe 2. Indeed, the metallic cylindrical shape of the needle upper part (blue curve) leads to a field aligned with the radial axis; and in between the needle and the ground plate (red curve), the field is mainly vertical. As the measurement is performed and acquired in real time, one can analyse the phase shift $\Delta\phi$ between the two curves. $\Delta\phi$ is here 90° in agreement with a typical *RC* circuit. When the applied voltage is increased over the threshold (> 16.5 kVrms, Fig.2b), the radial field remains linear (blue curve) with the applied voltage only for location 2 (close to the metal and far from the discharges). Nevertheless, the red curve presents a typical signature of the discharge once the threshold value is reached, both for positive and negative field. The corresponding peak values exceed 1 MV/m. Moreover the nominal field at 50 Hz has been increased by a factor 5 while the voltage is only doubled. This latter observation is due to modifications of the field direction induced by the DBD, towards a quasi totally horizontal field, along the sensitivity axis of the probe. Concerning the phase shift, the two signals are now in phase because the DBD transforms the previous *RC* configuration into a pure resistive electrical circuit.

The ability of the probe to measure each component of the field vector independently allows to analyse its temporal evolution in magnitude and orientation. The synchronized acquisition of the radial and longitudinal component, *Er* and *El*, leads to polarization trace on the field vector. Fig.3 gives an example of the vectorial trace of the field in location 1, for two different values of the applied voltage.

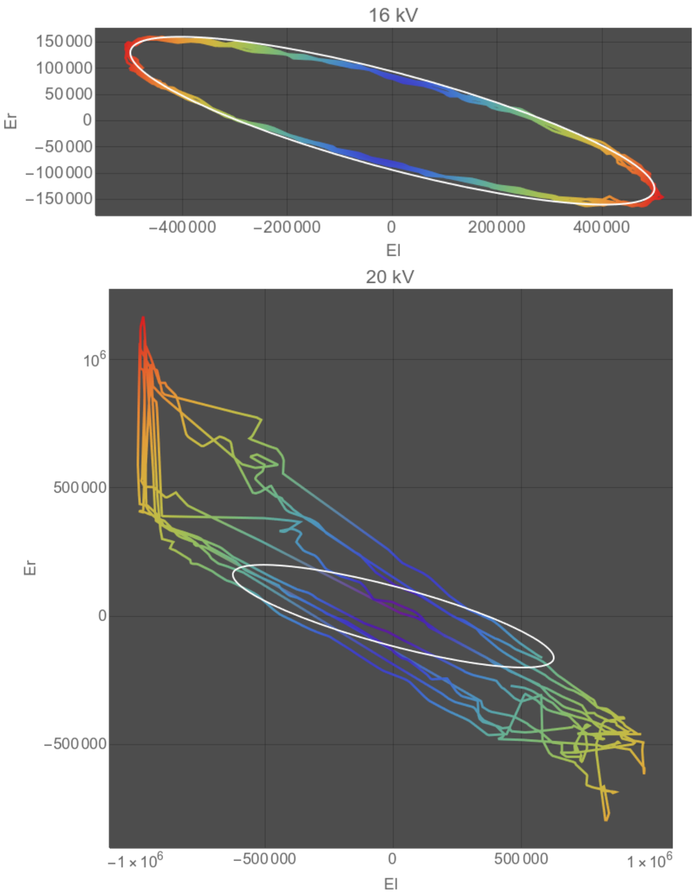


Fig. 3. a) Temporal trace of the field vector deduced from the measurement of Er and El, for an applied voltage of 16 kV, just below the threshold. The ellipse is the feeding curve. b) Temporal trace of the field vector deduced from the measurement of Er and El, for an applied voltage of 20 kV. The ellipse corresponds to the previous one scaled by a factor 20/16=1.25.

The expected signature in absence of DBD is an ellipse induced by the contribution of the radial field in zone 2 and 90° phase shifted of the vertical field in the capacitive zone.

On can notice a dramatic difference between the signature with and without DBD. In the presence of the DBD, the shape is defined by several almost straight lines. This illustrates a proportional link between *Er* and *El*, with linear coefficients depending on the temporal position in the waveform. The left upper zone is clearly associated to the discharge with a huge enhancement of the radial field up to more than 1 MV/m. For lower values of the field strength (center of Fig.3b), *Er* increases linearly together with *El*. The slope |*Er*/*El*| ranges from 0.62 to 1.16.

## 4. Conclusion

The performances of the EO probe allow the vectorial and real time analysis of the E-field induced by plasma sources. The properties of the field can be extracted in linear regime as well as for non-linear behaviour. All the properties of the probe will be explained during the conference: sensitivity, linearity, dynamics, vectorial selectivity, frequency bandwidth and so on. Numerous experimental analysis will be presented during the conference: DBD analysis, plasma jet characterization, influence of biological media on the operation of plasma source, ...

## 5. References


[1] A. Schutze, J. Y. Jeong, S. E. Babayan, J. Park, G. S. Selwyn, and R. F. Hicks, "*The atmospheric-pressure plasma jet: a review and comparison to other plasma sources*", EEE Transactions on Plasma Science, 26, 6, 1998.

[2] J. Hopwood, C. R.Guarnieri, S. J. Whitehair and J. J. Cuomo. "*Langmuir probe measurements of a radio frequency induction plasma*". Journal of Vacuum Science & Technology A: Vacuum, Surfaces, and Films, *11,*1, 152-156, 1993.

[3] R. Piejak, V. Godyak, and B. Alexandrovich. "*The electric field and current density in a low-pressure inductive discharge measured with different B-dot probes*." Journal of applied physics 81.8: 3416-3421, 1997.

[4] D. Vendor and R. W. Boswell. "*Numerical modeling of low-pressure RF plasmas.*" *I*EEE Transactions on Plasma Science 18.4: 725-732, 1990.

[5] Mason, Rodney J. "An electromagnetic field algorithm for 2D implicit plasma simulation." *Journal of Computational Physics* 71.2: 429-473, 1987.

[6] A. Jianming, X. Xie, and X-C. Zhang. "*Detection of broadband terahertz waves with a laser-induced plasma in gases.*" Physical review letters 97.10: 103903, 2006.

[7] F. Sanjuan, G. Gaborit and J.-L. Coutaz, "*Full electro-optic terahertz time-domain spectrometer for polarimetric studies*", Applied Optics, 57, 21, 6055-6060, 2018.

[8] G. Gaborit, A. Biciunas, M. Bernier and J. L. Coutaz, "*Emitting and Receiving Terahertz Vectorial Antennas Based on Cubic Electro-Optic Crystals*", IEEE Transactions on Terahertz Science and Technology, 5, 5, 2015.

[9] G. Gaborit, J. Dahdah, F. Lecoche, P. Jarrige, Y. Gaeremynck, E. Duraz, and L. Duvillaret. "*A nonperturbative electrooptic sensor for in situ electric discharge characterization*". IEEE Transactions on Plasma Science, 41(10), 2851-2857, 2013.

[10] G. Gaborit, J. Dahdah, F. Lecoche, P. Jarrige, E. Duraz, C. Volat and L. Duvillaret. "*Single shot and vectorial characterization of intense electric field in various environments with pigtailed electrooptic probe*". IEEE Transactions on Plasma Science, *42*(5), 1265-1273, 2014.